Applied Geochemistry 208 (2026) 106974

Contents lists available at ScienceDirect

Applied Geochemistry

journal homepage: www.elsevier.com/locate/apgeochem

Phosphate and nitrate isotope responses to lateral plume mixing and nutrient turnover downstream of a wastewater discharge

Daren C. Gooddy [a,b,*], Michael J. Bowes [a], Alexandra V.E. O'Brien [a], David J.E. Nicholls [a], Andi C. Smith [c], James P.R. Sorensen [d], Patrick Harrison [d], Stefan Krause [e]

[a] UK Centre for Ecology and Hydrology, Maclean Building, Wallingford, Oxon, OX10 8BB, UK
[b] Lancaster Environment Centre, University of Lancaster, Lancaster, LA1 4YQ, UK
[c] British Geological Survey, Keyworth, Nottingham, NG12 5GG, UK
[d] British Geological Survey, Maclean Building, Wallingford, Oxon, OX10 8BB, UK
[e] University of Birmingham, GEES, Birmingham, B15 2TT, UK

ARTICLE INFO

Editorial handling by Elisa Sacchi

Keywords:
Phosphate isotopes
Nitrate isotopes
Wastewater effluent plumes
Hydrodynamic mixing
River nutrient processing

ABSTRACT

Wastewater treatment works (WwTW) are major point sources of nutrients to rivers, but interpretation of downstream isotope signals is complicated where hydrodynamic mixing and in-stream biogeochemical processing occur over similar spatial scales. Here, we combine phosphate oxygen isotopes ($\delta^{18}O\text{-}PO_4$), nitrate nitrogen and oxygen isotopes ($\delta^{15}N\text{–}NO_3$ and $\delta^{18}O\text{–}NO_3$), and nutrient concentrations to investigate nutrient behaviour over a short River Thames, UK reach downstream of a WwTW discharge. The study resolves a high-resolution spatial pattern from a single sampling survey and is framed within a two-dimensional mixing context, in which effluent-influenced water and background river water are transported downstream in parallel rather than as a laterally well-mixed one-dimensional system. Phosphate concentrations and $\delta^{18}O\text{-}PO_4$ values showed a strong response to the effluent input. Near the outfall, isotope compositions were broadly consistent with conservative mixing between effluent and river phosphate, with first-order estimates suggesting that effluent-derived phosphate contributed approximately 20–55% of the local dissolved inorganic phosphate pool at plume-influenced sampling points. Further downstream, several $\delta^{18}O\text{-}PO_4$ values were close to the independently calculated temperature-dependent equilibrium composition of approximately 17.2‰, consistent with possible biological isotope resetting of phosphate within the reach. However, because travel times and turnover rates were not directly measured, this convergence is interpreted as evidence for short-reach isotope resetting rather than as a quantified rate of biological turnover. A pronounced low $\delta^{18}O\text{-}PO_4$ value at approximately 220 m downstream fell outside the range predicted using the measured effluent end member, indicating end-member uncertainty or plume heterogeneity within the wastewater-influenced water mass. In contrast, nitrate concentrations and isotope compositions showed little spatial variation downstream of the discharge. $\delta^{15}N\text{–}NO_3$ and $\delta^{18}O\text{–}NO_3$ displayed no coupled downstream enrichment, indicating no detectable isotopic evidence for substantial denitrification over the sampled reach and hydrological conditions. However, the large background nitrate pool means that local nitrogen transformations, including nitrification, assimilation or localised denitrification, may have been difficult to resolve. These contrasting isotope responses show that phosphate was sensitive to both local plume structure and possible biological isotope resetting, whereas nitrate primarily reflected buffering by a large background nitrate pool. More broadly, the results demonstrate that interpretation of river nutrient isotope signals below point-source inputs requires explicit consideration of lateral hydrodynamic structure, end-member uncertainty and nutrient-specific reactivity.

1. Introduction

Rivers receiving treated wastewater effluents experience strong physical and biogeochemical perturbations that alter nutrient concentrations, speciation and cycling over short spatial scales (Carpenter et al., 1998; Hilton et al., 2006). Understanding how nutrients are

* Corresponding author. UK Centre for Ecology and Hydrology, Maclean Building, Wallingford, Oxon, OX10 8BB, UK.
E-mail address: dargoo@ceh.ac.uk (D.C. Gooddy).

https://doi.org/10.1016/j.apgeochem.2026.106974
Received 15 May 2026; Received in revised form 17 June 2026; Accepted 8 July 2026
Available online 9 July 2026

transported and transformed downstream of point sources is therefore central to environmental geochemistry, river monitoring and nutrient management (Jarvie et al., 2006; Bowes et al., 2014; Water Framework Directive Council of European Communities, 2000). Interpretation of downstream nutrient signals remains challenging, however, because observed changes commonly reflect the combined effects of source inputs, hydrodynamic mixing, plume structure and in-stream processing. Receiving rivers are often interpreted as laterally well-mixed one-dimensional systems in which downstream distance alone describes chemical evolution. In reality, point-source discharges can form laterally confined plumes that persist over hundreds of metres, allowing distinct water masses to coexist at the same downstream location (Volkmar et al., 2011; Palmer-Felgate et al., 2010). Under such conditions, chemical and isotopic patterns cannot be interpreted from longitudinal trends alone.

Stable isotopes provide a powerful basis for evaluating the relative influence of physical mixing and biogeochemical transformation because different nutrient species respond differently to these processes (Kendall, 1998; Kendall et al., 2007). Nitrate nitrogen and oxygen isotopes ($\delta^{15}N–NO_3$ and $\delta^{18}O–NO_3$) primarily record source signatures and, unless nitrate is actively removed, tend to behave conservatively during transport (Böhlke and Denver, 1995; Wassenaar, 1995; Venkiteswaran et al., 2019; Matiatos et al., 2021). In contrast, phosphate oxygen isotopes ($\delta^{18}O\text{-}PO_4$) are sensitive to biological cycling because oxygen exchange between phosphate and water occurs only during enzymatically mediated reactions (Blake et al., 1997, 2005; McLaughlin et al., 2013; Davies et al., 2014). As a result, $\delta^{18}O\text{-}PO_4$ can retain source-related information during conservative transport, but may also shift from source-dependent compositions towards a temperature-dependent equilibrium with ambient water where biological uptake, release and enzymatically mediated oxygen exchange occur (Chang and Blake, 2015; McLaughlin et al., 2006; Davies et al., 2014). This means that phosphate oxygen isotopes are not necessarily conservative during downstream transport, particularly where biological cycling and hydrodynamic mixing operate over similar spatial scales. Used together, nitrate and phosphate isotopes therefore offer complementary insight into nutrient behaviour: nitrate mainly constrains source and dilution, whereas phosphate can reflect both hydrodynamic mixing and biological turnover. The challenge is that these isotope signals must be interpreted within the hydrodynamic structure of the receiving system, particularly where incomplete lateral mixing causes individual samples to represent different water masses.

Recent studies have expanded the application of phosphate oxygen isotopes to phosphorus source apportionment across catchment to global scales, including through multi-model and Bayesian mixing approaches (Wang et al., 2023, 2024). Recent methodological and synthesis work has also highlighted both the potential and the interpretive challenges of $\delta^{18}O\text{-}PO_4$, including end-member characterisation, analytical comparability, deviations from equilibrium and the difficulty of separating source signals from biological cycling in complex environmental systems (Nisbeth et al., 2022; von Sperber et al., 2023; Pfahler et al., 2024). These developments highlight the growing value of $\delta^{18}O\text{-}PO_4$ as a tracer of phosphorus sources and cycling, but also emphasise the need to interpret phosphate isotope data within appropriate hydrodynamic and biogeochemical context.

Despite this potential, relatively few studies have applied multi-nutrient isotope approaches at spatial resolutions sufficient to resolve near-field wastewater mixing and transformation. Where isotopes are used in river systems, interpretations often rely on longitudinal trends and may implicitly assume complete lateral mixing (Gooddy et al., 2016; Tonderski et al., 2017). Under conditions where wastewater effluent forms a laterally confined plume that remains restricted to part of the channel rather than mixing across the full width, samples collected at the same downstream distance may represent fundamentally different water masses, and end-member mixing models are only valid at the scale of individual samples (Volkmar et al., 2011). For reactive nutrients such as phosphate, biological processing may also vary within the plume itself, leading to spatial heterogeneity that cannot be captured by sparse or single-bank sampling (Gruau et al., 2005; Young et al., 2009; Gooddy et al., 2018).

Here, we apply a combined isotope approach using $\delta^{18}O\text{-}PO_4$, $\delta^{15}N–NO_3$ and $\delta^{18}O–NO_3$, together with nutrient concentrations, to investigate nutrient behaviour downstream of a wastewater treatment works discharge over a 400 m river reach. The study is analysed within a two-dimensional framework that allows for incomplete lateral mixing between effluent-influenced water and background river water transported downstream in parallel. Within this framework, end-member mixing provides a first-order description of the isotopic composition of individual samples as a function of local plume contribution, while comparison with the temperature-dependent equilibrium composition of phosphate provides a basis for assessing whether $\delta^{18}O\text{-}PO_4$ values are consistent with biological isotope resetting. The aim is not to derive a reach-scale turnover rate, but to test how hydrodynamic structure, end-member uncertainty and nutrient-specific reactivity affect the interpretation of isotope signals below a wastewater input. The specific objectives are to assess where conservative mixing provides an adequate explanation for the observed isotope patterns, evaluate where phosphate isotope compositions are consistent with biological cycling, and compare this response with the more conservative behaviour of nitrate under the sampled hydrological conditions.

2. Study site, sampling design and sample handling

The study was conducted on the River Thames downstream of the Pangbourne Wastewater Treatment Works discharge near Reading, UK (51.488° N, 1.077° W). The reach was selected to resolve near-field mixing and nutrient isotope behaviour at high spatial resolution

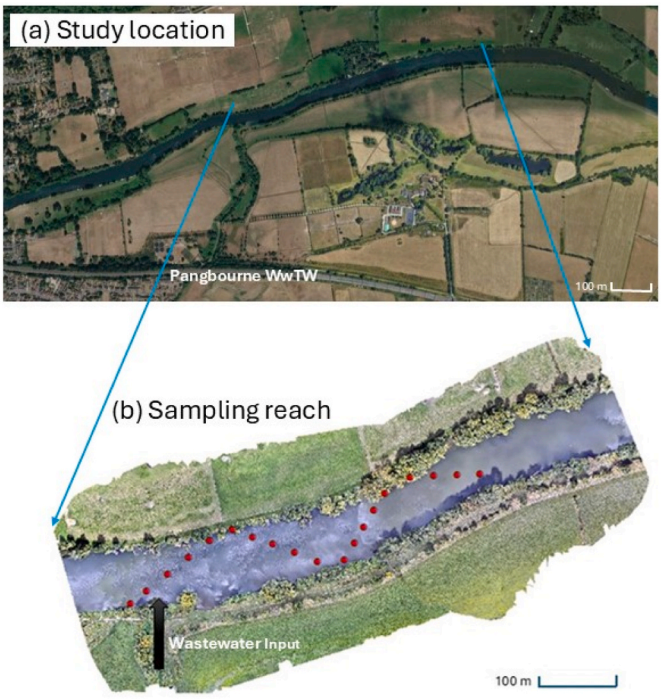

Fig. 1. Location and sampling design for the study reach. (a) Location of the River Thames study area downstream of Pangbourne Wastewater Treatment Works near Reading, UK. (b) Drone photograph taken on the day of sampling showing the WwTW discharge, the downstream sampling reach and individual sampling points. Samples were collected upstream of the discharge and at multiple downstream locations, with right-bank, mid-channel and left-bank positions sampled where feasible. *Map data ©2026 Google, Imagery ©2026 CNES/Airbus, Maxar Technologies.*

downstream of a single point-source input (Fig. 1). Sampling was undertaken at 11:00 on 9 September 2025 and therefore represents a spatially detailed snapshot under one set of hydrological and operational conditions.

River discharge data from the Environment Agency gauging station at Reading (NRFA station 39130), approximately 10 km downstream of the sampling reach, indicate flows of approximately 60–70 $m^3 s^{-1}$ at the time of sampling. The WwTW discharge rate was not measured during the survey, so the relative magnitude of the effluent input is assessed here from concentration and isotope contrasts rather than from a contemporaneous discharge-weighted mass balance. Sampling was not timed to target a specific diurnal phase of WwTW operation, but was undertaken as a short-duration spatial survey to minimise temporal change during sample collection. The river is approximately 50 m wide through the study reach, with water depths of around 2 m in the maintained navigation channel.

The maximum permitted daily discharge volume for the works is 1500 $m^3 d^{-1}$, equivalent to an average discharge of approximately 0.017 $m^3 s^{-1}$ if spread uniformly over 24 h, although the actual discharge at the time of sampling was not measured.

The reach extends approximately 400 m downstream from the effluent stream and provides a hydrologically simple but chemically dynamic setting in which the influence of a single point source can be examined. The WwTW effluent is discharged continuously into the river through a single outlet located on the right bank, facing downstream. Given this bank-side discharge location and the short spatial scale considered, the sampling design was intended to test whether effluent-derived water remained laterally structured within the channel rather than mixing rapidly across the full river width.

Sampling targeted both downstream change and lateral variability. One upstream sample was collected to characterise background river conditions prior to effluent input, and one WwTW effluent sample (SW-20) was collected directly from the discharge to define the measured wastewater end member. The upstream sample was collected on the same bank as the WwTW discharge and is treated as the local upstream river end member for the mixing calculations. A full upstream transverse transect was not collected, so possible upstream cross-channel heterogeneity cannot be fully evaluated. However, given the downstream-facing discharge outlet and normal downstream river flow at the time of sampling, direct WwTW influence immediately upstream of the discharge is considered unlikely.

Downstream samples were collected to approximately 400 m from the outfall, with right-bank, mid-channel and left-bank positions sampled where feasible from a canoe. The sampling pattern was not intended to represent a set of formal discharge-weighted cross-sections. Instead, it was designed to intercept different local water masses along and across the expected plume pathway, while allowing practical sampling from a canoe under field conditions. The resulting curved sampling pattern reflects this objective: to combine longitudinal coverage with repeated lateral contrasts, rather than to assume that each downstream distance represented a laterally mixed river cross-section. No dye tracing, ADCP survey, or independent visual plume-tracking was undertaken during the survey, and the plume interpretation is therefore based on the outfall geometry, spatial sampling pattern, drone imagery and the observed chemical and isotopic gradients.

At each sampling point, 10 L grab samples were collected in polyethylene carboys from the upper water column, with the lip of the carboy approximately 10 cm below the river surface. The large sample volume was required to provide sufficient phosphate for $\delta^{18}O\text{-}PO_4$ analysis following brucite precipitation. Samples were collected carefully from the canoe to avoid disturbance of bed sediment and to capture the local water mass represented by each sampling position. Subsamples for nutrient concentrations, $\delta^{18}O–H_2O$ and nitrate isotope analysis were taken from these carboys. Vertical profiles were not collected, so depth-related variation cannot be assessed directly. However, the sampling design focused on lateral plume structure, which was expected to be the dominant source of spatial variability given the bank-side discharge and the width of the channel.

This design allowed direct evaluation of cross-channel heterogeneity and avoided reliance on the assumption of complete lateral mixing. However, the upstream and effluent samples should be interpreted as discrete end-member observations from the time of sampling rather than as full characterisations of temporal variability in either the river or the effluent. This is particularly relevant for the isotope mixing calculations, which are used here as first-order estimates of local plume contribution rather than temporally integrated source apportionments.

Samples were stored cold and in the dark prior to processing. All samples were filtered in the field or immediately upon return to the laboratory using 0.45 μm membrane filters to remove particulate material and isolate the dissolved nutrient fraction following the methods ofBowes et al. (2018). Subsamples for nutrient concentration analysis were refrigerated and analysed within recommended holding times, while subsamples for isotope analysis were stored frozen until preparation. The remaining sample volume was used for phosphate isotope preparation.

All samples were analysed for soluble reactive phosphorus (SRP) and for nitrate (NO_3^-), nitrite (NO_2^-), and ammonium (NH_4^+) concentrations. Isotopic analyses included phosphate oxygen isotopes ($\delta^{18}O\text{-}PO_4$), nitrate nitrogen isotopes ($\delta^{15}N–NO_3$), and nitrate oxygen isotopes ($\delta^{18}O–NO_3$). Together, these parameters provide a basis for comparing the behaviour of phosphate and nitrate under the same hydrodynamic conditions.

3. Analytical methods

3.1. Water analysis

Soluble reactive phosphorus (SRP) was determined colorimetrically using the molybdenum blue method following standard procedures (Murphy and Riley, 1962) as modified by Neal et al. (2000). Total Dissolved Phosphorus was determined on filtered samples by the method of Eisenreich et al. (1975). Total Phosphorus was determined on unfiltered samples using the same method. Ammonium (NH_4^+) concentrations were measured colorimetrically using the Berthelot reaction (indophenol blue). Nitrate (NO_3^-) and nitrite (NO_2^-) were measured using ion chromatography. Analytical precision for nutrient concentrations was better than ±5%.

Precipitated Ag_3PO_4 was analysed by weighing 200 μg of dried and ground Ag_3PO_4 into a capsule, in duplicate. During high-temperature pyrolysis in the presence of carbon, oxygen from Ag_3PO_4 is quantitatively converted to carbon monoxide (CO), which is then analysed by isotope ratio mass spectrometry. The sample was converted to CO using an Elementar PYRO cube elemental analyser at 1450 °C in the presence of carbon sources, and product CO was analysed on an Elementar Vision IRMS. The $\delta^{18}O\text{-}PO_4$ values were put on the international reference scale using two Ag_3PO_4 standards, B2207 and USGS80, and an internal Ag_3PO_4 standard, ALFA-2 (ALFA-2 = $\delta^{18}O$ VSMOW value of +14.2‰), used as a check standard. Duplicate repeats had a precision $\sigma \leq 0.3$‰. Sample purity was assessed by determining the CO yield compared with the yield of Ag_3PO_4 standards. Samples were rejected where the CO yield differed by more than 3% from the expected oxygen yield of Ag_3PO_4. This threshold was used as an internal QA criterion to screen for incomplete conversion or sample impurity, rather than as a universal convention across all $\delta^{18}O\text{-}PO_4$ laboratories.

Nitrate isotope analysis ($\delta^{18}O–NO_3$ and $\delta^{15}N–NO_3$) was undertaken on <3 ml of filtered water sample using the TiCl reduction method of Altabet et al. (2019). Briefly, the sample was added to a 40 ml glass reaction vessel, 50 μl of 10% HCl was added to reduce the pH, the sample was then capped with a septum cap before 140 μl of preconditioned TiCl was injected, to convert dissolved NO_3 to N_2O gas for analysis. Product N_2O was analysed on an Elementar Vision IRMS. The $\delta^{18}O–NO_3$ and $\delta^{15}N–NO_3$ values were validated against international standards

USGS34, USGS35 and IAEA NO3. Duplicate sample repeats had a $\delta^{18}O–NO_3$ precision $\sigma \leq 0.6‰$ and for $\delta^{15}N–NO_3$ a precision $\sigma \leq 0.4‰$.

To enable the calculation of the phosphate oxygen isotope equilibrium, water oxygen isotope analysis ($\delta^{18}O–H_2O$) was undertaken. Analysis was performed on an Isoprime Aquaprep coupled to an Isoprime 100 dual-inlet mass spectrometer through the headspace CO_2 equilibration with the water samples. Isotope ratios are reported as $\delta^{18}O–H_2O$ versus VSMOW, based on comparison with laboratory standards calibrated against IAEA standards VSMOW and SLAP, with analytical precision typically $\sigma \leq 0.05‰$.

3.2. Calculation of phosphate oxygen isotope equilibrium

The temperature-dependent equilibrium composition of phosphate oxygen isotopes was calculated to provide an independent reference value against which measured $\delta^{18}O\text{-}PO_4$ compositions could be compared. The calculation used the measured $\delta^{18}O–H_2O$ composition of each water sample, the water temperature measured during sampling, and the equilibrium fractionation relationship for phosphate and water reported by Chang and Blake (2015):

$$\delta^{18}O_{PO4} = \left(\delta^{18}O_{H2O} + 1000\right) \times e^{\left[14.43\times\left(10^3/T\right)-26.54\right]/1000} - 1000 \quad (1)$$

where $\delta^{18}O\text{-}PO_4(eq)$ is the calculated equilibrium composition of phosphate, $\delta^{18}O–H_2O$ is the measured water isotope composition, and T is absolute temperature in degrees Kelvin. Water temperature at the time of sampling was 17.7 °C (290.85 K). Because $\delta^{18}O–H_2O$ varied only slightly across the reach, calculated equilibrium $\delta^{18}O\text{-}PO_4$ values also varied over a narrow range, with values close to 17.2‰ for most river samples.

The calculated equilibrium value is used here as a reference for assessing whether measured $\delta^{18}O\text{-}PO_4$ values are close to, or displaced from, the composition expected after biological isotope exchange with ambient river water. It is not used to calculate a phosphate turnover rate, because travel times and isotope exchange rates were not directly measured during the survey.

3.3. End-member mixing model for $\delta^{18}O\text{-}PO_4$

To provide a first-order estimate of the contribution of wastewater-derived phosphate to the local river dissolved inorganic phosphate (DIP) pool, a two-end-member mixing model was applied to the phosphate oxygen isotope data. More complex multi-end-member and Bayesian mixing approaches have been applied successfully to $\delta^{18}O\text{-}PO_4$ datasets at catchment and continental scales (Wang et al., 2023, 2024). However, the objective here was not regional source apportionment, but evaluation of local plume interception and initial isotope conditions within a short wastewater-affected reach. A simple two-end-member framework was therefore used as a transparent reference case against which phosphate isotope behaviour could be assessed.

The model assumes conservative mixing between phosphate derived from upstream river water and phosphate derived from the WwTW effluent, prior to any biological oxygen isotope exchange between phosphate and water. The isotopic composition of mixed phosphate is given by:

$$\delta^{18}O_{P,mix} = f_w\delta^{18}O_{P,w} + (1-f_w)\delta^{18}O_{P,R} \quad (2)$$

Rearranging this expression allows direct calculation of the apparent effluent contribution:

$$f_w = \frac{\delta^{18}O_{P,obs} - \delta^{18}O_{P,R}}{\delta^{18}O_{P,w} - \delta^{18}O_{P,R}} \quad (3)$$

where $\delta^{18}O_{P,mix}$ is the predicted phosphate oxygen isotope composition of a conservative mixture, $\delta^{18}O_{p,obs}$ is the measured value, $\delta^{18}O_{P,R}$ is the upstream river end-member value, $\delta^{18}O_{P,W}$ is the isotope composition of the effluent phosphate value, and f is the fraction of phosphate derived from the WwTW.

The resulting value of *f* should be interpreted as an apparent local effluent phosphate fraction for the sampled water mass, rather than as a reach-averaged or cross-section-averaged contribution. This distinction is important because the effluent plume was laterally structured, so samples collected at the same downstream distance may represent different mixtures of effluent-influenced water and background river water.

The model is intentionally conservative and does not include biological isotope exchange. Biological processing is evaluated separately by comparing measured $\delta^{18}O\text{-}PO_4$ values with the independently calculated temperature-dependent equilibrium composition for phosphate in ambient river water (Blake et al., 2005; Chang and Blake, 2015). In this sense, the mixing model defines the range of $\delta^{18}O\text{-}PO_4$ values expected from conservative mixing alone, while comparison with equilibrium provides a basis for assessing whether individual samples are consistent with subsequent isotope resetting.

Because the wastewater end member was represented by a single grab sample, the calculated effluent fractions are sensitive to the assumed $\delta^{18}O\text{-}PO_4$ composition of effluent phosphate. The model results are therefore treated as first-order estimates rather than precise source apportionments. Where measured river $\delta^{18}O\text{-}PO_4$ values fall outside the range defined by the upstream and measured effluent end members, these samples are interpreted as indicating end-member variability or plume heterogeneity, rather than being forced into the conservative mixing calculation.

4. Results

Across all samples (Table 1), $\delta^{18}O\text{-}PO_4$ ranged from 12.5 to 17.9‰ (mean 16.7‰), while nitrate isotope compositions varied from 12.9 to 20.5‰ for $\delta^{15}N–NO_3$ and from 1.6 to 8.6‰ for $\delta^{18}O–NO_3$, with river water $\delta^{18}O$ remaining stable (−6.88 to −5.98‰). Soluble reactive phosphorus ranged from 240 to 885 μg L^{-1} P (mean 277 μg L^{-1}), total dissolved phosphorus from 269 to 998 μg L^{-1} P (mean 313 μg L^{-1}), and total phosphorus from 291 to 1050 μg L^{-1} P (mean 371 μg L^{-1}), while nitrate concentrations were consistently high (40.7-119 mg L^{-1} NO_3^- mean 44.9 mg L^{-1}) and ammonium remained low except in the effluent (0.010-0.306 mg L^{-1} NH_4^+).

4.1. Phosphorus concentrations and phosphate oxygen isotopes

Total phosphorus (TP), total dissolved phosphorus (TDP) and soluble reactive phosphorus (SRP) showed contrasting spatial patterns along the study reach (Fig. 2). The WwTW effluent sample contained markedly elevated TP (1050 μg L^{-1} P), TDP (998 μg L^{-1} P) and SRP (885 μg L^{-1} P) relative to the river samples. River TP concentrations ranged from approximately 291 to 477 μg L^{-1} P, with the highest values occurring at discrete downstream locations rather than showing a simple monotonic downstream decrease. TDP showed a similar, although less pronounced,

Table 1
Summary statistics of nutrient concentrations and isotope compositions along the study reach.

Parameter	Min	Max	Mean	Stdev
Phosphate $\delta^{18}O$ (‰)	12.5	17.9	16.7	1.25
Phosphate $\delta^{18}O$ equilibrium (‰)	16.3	17.2	17.1	0.20
Nitrate $\delta^{15}N$ (‰)	12.9	20.5	14.8	1.55
Nitrate $\delta^{18}O$ (‰)	1.6	8.6	5.1	1.7
Water $\delta^{18}O$ (‰)	−6.88	−5.98	−6.05	0.19
Soluble reactive P (μg L^{-1} P)	240	885	277	143
Total dissolved P (μg L^{-1} P)	269	998	313	159
Total P (μg L^{-1} P)	291	1050	371	167
NH_4^+ (mg L^{-1})	0.01	0.31	0.03	0.07
NO_3^- (mg L^{-1})	40.7	119	44.9	17.4

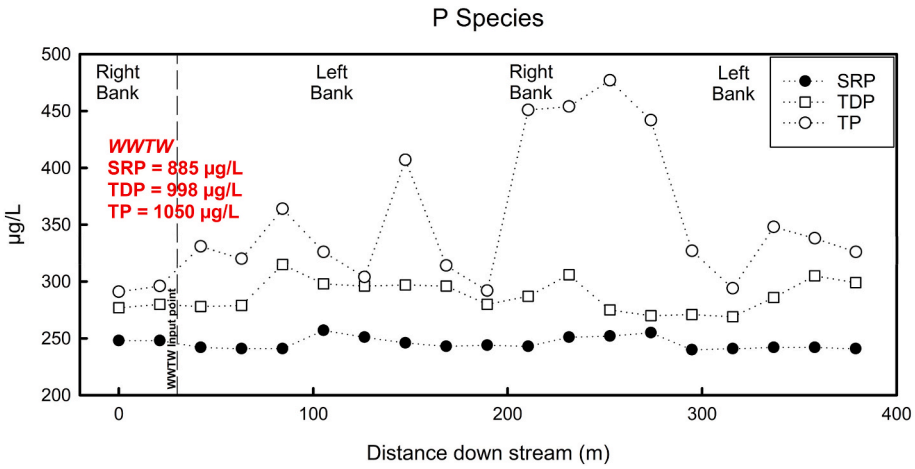

Fig. 2. Downstream evolution of phosphorus species.

spatial pattern. In contrast, SRP concentrations in the river varied over a narrower range, approximately 240–257 µg L^{-1} P.

The $\delta^{18}O\text{-}PO_4$ measurements represent phosphate isolated from filtered samples and therefore relate most directly to the dissolved inorganic phosphate fraction rather than to bulk TP. The contrasting behaviour of TP, TDP and SRP is considered further in the Discussion, particularly in relation to particulate or colloidal phosphorus and the interpretation of plume structure.

Phosphate oxygen isotope compositions also varied along the sampled reach (Fig. 3). Upstream river phosphate was characterised by $\delta^{18}O\text{-}PO_4$ values close to 18‰, whereas the measured effluent phosphate end member was isotopically lighter, at approximately 14–15‰. Immediately downstream of the outfall, river $\delta^{18}O\text{-}PO_4$ values shifted toward the effluent composition, producing intermediate values between the measured river and effluent end members. This pattern is consistent with local mixing between background river phosphate and effluent-derived phosphate in the near field of the discharge.

A pronounced low $\delta^{18}O\text{-}PO_4$ value of 12.5‰ was observed at approximately 220 m downstream. This value is lower than the measured effluent end member collected during the survey and therefore falls outside the range predicted by conservative mixing using the measured upstream and effluent samples. The same location also coincided with elevated TDP and TP concentrations relative to most other river samples. This sample is therefore identified as an out-of-envelope value in relation to the measured end members. Possible explanations, including effluent end-member variability, plume heterogeneity, analytical uncertainty, additional phosphorus inputs, and local biogeochemical effects, are considered in Section 5.2.

Measured $\delta^{18}O\text{-}PO_4$ values were compared with the calculated temperature-dependent equilibrium composition shown in Fig. 3. Most river samples were close to the calculated equilibrium value, while a small number of samples, including the low value at approximately 220 m downstream, showed larger offsets. The significance of these offsets depends on analytical uncertainty, uncertainty in the calculated equilibrium value, and uncertainty in the effluent end-member composition, and is considered further in Section 5.2.

Application of the two-end-member mixing model provided first-order estimates of the apparent local contribution of effluent-derived phosphate to the sampled dissolved inorganic phosphate pool (Fig. 4). For samples falling within the measured upstream–effluent isotope range, calculated effluent contributions were generally within the range of approximately 20–55%. The calculated fractions varied substantially between adjacent sampling positions and did not show a simple downstream dilution trend. This variability is consistent with the sampling of different local water masses within a laterally structured plume. Samples indicated by arrows fall outside the model bounds defined by the measured end members, highlighting the sensitivity of the calculation to end-member composition. These samples are therefore treated as boundary-condition cases rather than precise fractional contributions.

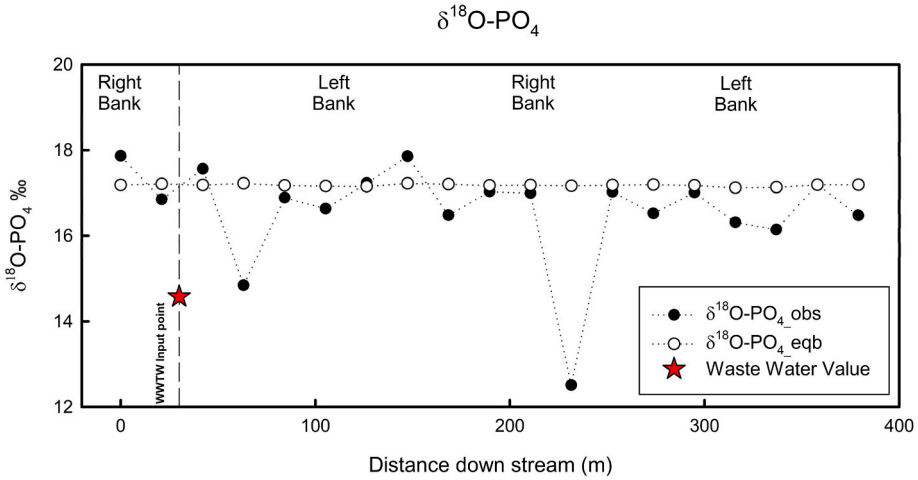

Fig. 3. Downstream evolution of phosphate oxygen isotopes ($\delta^{18}O\text{-}PO_4$) in upstream river water, WwTW effluent, and downstream samples along the study reach. The dashed line shows the temperature-dependent equilibrium value.

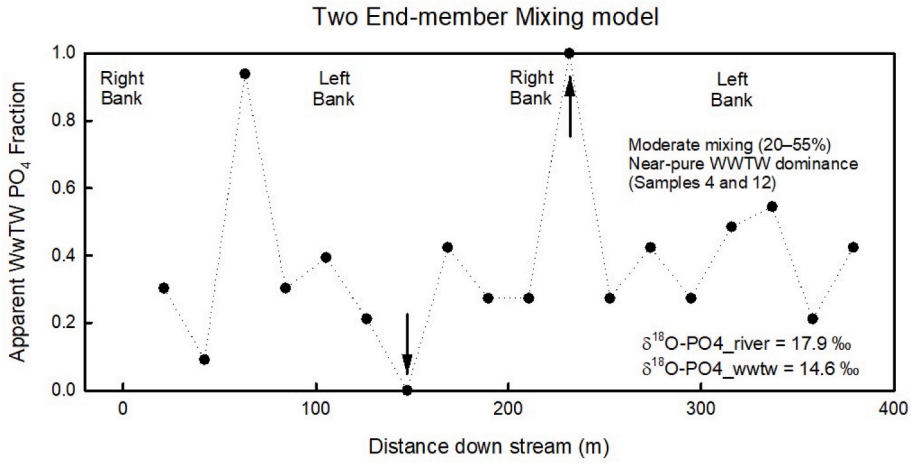

Fig. 4. Apparent local contribution of effluent-derived phosphate estimated from a two-end-member δ^{18}O-PO_4 mixing model. Values represent the sampled water mass and should not be interpreted as cross-section-averaged effluent contributions. Upward and downward arrows indicate samples that fall outside the model bounds defined by the measured upstream river and WwTW effluent end members. These boundary-condition cases reflect sensitivity to the selected end-member compositions and are interpreted as evidence of end-member uncertainty or plume heterogeneity rather than as precise fractional estimates.

4.2. Nitrogen concentrations and nitrate isotopes

Nitrate concentrations in the river were high and relatively uniform along the sampled reach, with values consistently around 40–41 mg NO_3 L^{-1} (Fig. 5). Nitrite concentrations were below detection limits in all river samples, and ammonium concentrations were very low, generally <0.02 mg NH_4 L^{-1}. This indicates that dissolved inorganic nitrogen in the river was dominated by nitrate at the time of sampling. In contrast, the WwTW sample (SW-20) showed a distinct nitrogen composition, with substantially elevated nitrate concentration and elevated ammonium relative to the river samples.

Despite the contrast between effluent and river chemistry, no systematic downstream increase in nitrate or ammonium concentrations was observed in the river following the discharge. River concentrations instead remained stable within a narrow range, indicating that the effluent nitrogen signal was not clearly resolved against the large background nitrate pool over the spatial scale and hydrological conditions sampled.

Nitrate isotope compositions in the river also showed limited spatial variability. δ^{15}N–NO_3 values in river samples generally ranged between approximately +13 and + 15‰, while δ^{18}O–NO_3 values clustered between about +2 and + 8‰ (Fig. 6). These values are consistent with a nitrate pool dominated by upstream source inputs and within-reach transport, with little measurable perturbation from the WwTW discharge. In contrast, the WwTW effluent sample exhibited elevated δ^{15}N–NO_3 of approximately +20.5‰ and slightly higher δ^{18}O–NO_3 values, consistent with sewage-derived nitrogen that has undergone processing within the treatment system.

No systematic downstream enrichment in δ^{15}N–NO_3 was observed following the WwTW discharge. River δ^{15}N–NO_3 averaged 14.2‰, with a 3σ range of 2.1‰. δ^{18}O–NO_3 showed greater variability, averaging 5.1‰ with a 3σ range of 5.1‰, and included one downstream value similar in magnitude to the WwTW effluent value near the location of the low δ^{18}O-PO_4 sample. However, this was not accompanied by a corresponding enrichment in δ^{15}N–NO_3. The nitrate isotope data therefore show no coupled downstream increase in δ^{15}N–NO_3 and δ^{18}O–NO_3 that would provide isotopic evidence for substantial denitrification over the sampled reach.

Overall, the nitrogen concentration and isotope data indicate that nitrate behaved much more conservatively than phosphate over the study reach. The WwTW effluent was chemically and isotopically distinct, but its signal was strongly buffered by the large background nitrate pool in the river. This provides a comparatively stable nitrogen isotope framework against which the more spatially variable phosphate

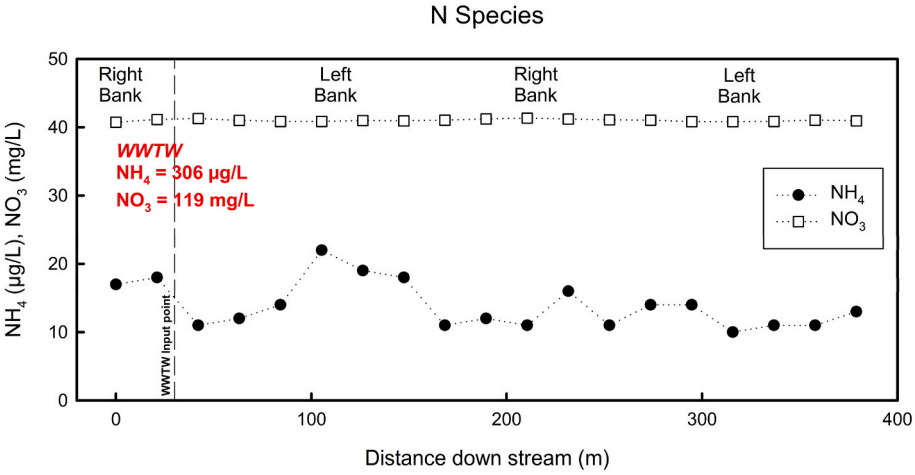

Fig. 5. Downstream evolution of nitrogen species. Concentrations of nitrate (NO_3) and ammonium (NH_4) in upstream river water, WwTW effluent, and downstream samples along the study reach. Nitrite was below detection in river samples.

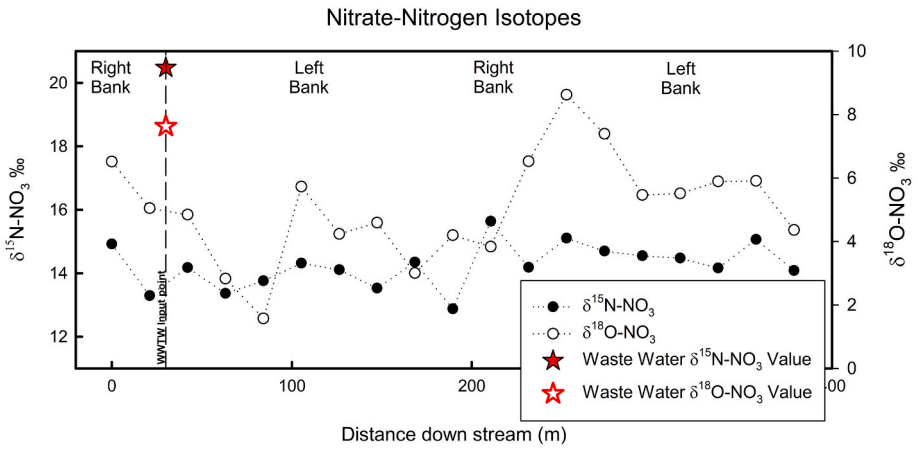

Fig. 6. Downstream evolution of nitrate isotopes ($\delta^{15}N–NO_3$ and $\delta^{18}O–NO_3$) in upstream river water, WwTW effluent, and downstream samples along the study reach.

response can be interpreted.

5. Discussion

5.1. Hydrodynamic control and plume structure

The combined concentration and isotope data indicate that hydrodynamic structure exerted a strong control on nutrient behaviour downstream of the WwTW. Rather than becoming rapidly mixed across the full channel width, the effluent appears to have remained as a laterally structured, right-bank plume over the sampled reach (Fig. 7a). Under these conditions, effluent-influenced water and background river water can be transported downstream in parallel, so downstream distance alone is insufficient to describe water-mass evolution or interpret isotope patterns. This is particularly important for the phosphate dataset, where spatial variability in TP, TDP and $\delta^{18}O\text{-}PO_4$ is more readily explained by interception of plume-influenced water masses than by a simple one-dimensional downstream trend.

The persistence of lateral heterogeneity over several hundred metres highlights that near-field effluent mixing can be slower than is often assumed when river reaches are treated as laterally well mixed. Longitudinal dilution may occur while cross-channel homogenisation remains incomplete, particularly where a bank-side discharge enters a relatively wide channel. In this study, the right-bank location of the discharge, the approximately 50 m channel width, the lateral sampling pattern, and the spatial variability in phosphorus concentrations and $\delta^{18}O\text{-}PO_4$ all support interpretation of a laterally structured plume. As a result, chemical and isotopic gradients may persist across the channel even where longitudinal concentration changes appear weak.

This hydrodynamic context helps explain the contrasting responses of nitrate and phosphate to the effluent input. Nitrate concentrations in the river showed little spatial variability, not necessarily because plume water was absent from downstream samples, but because the background nitrate pool was large and the effluent contribution did not measurably perturb the bulk river nitrate signal under the sampled conditions. Phosphate concentrations and isotope compositions, in

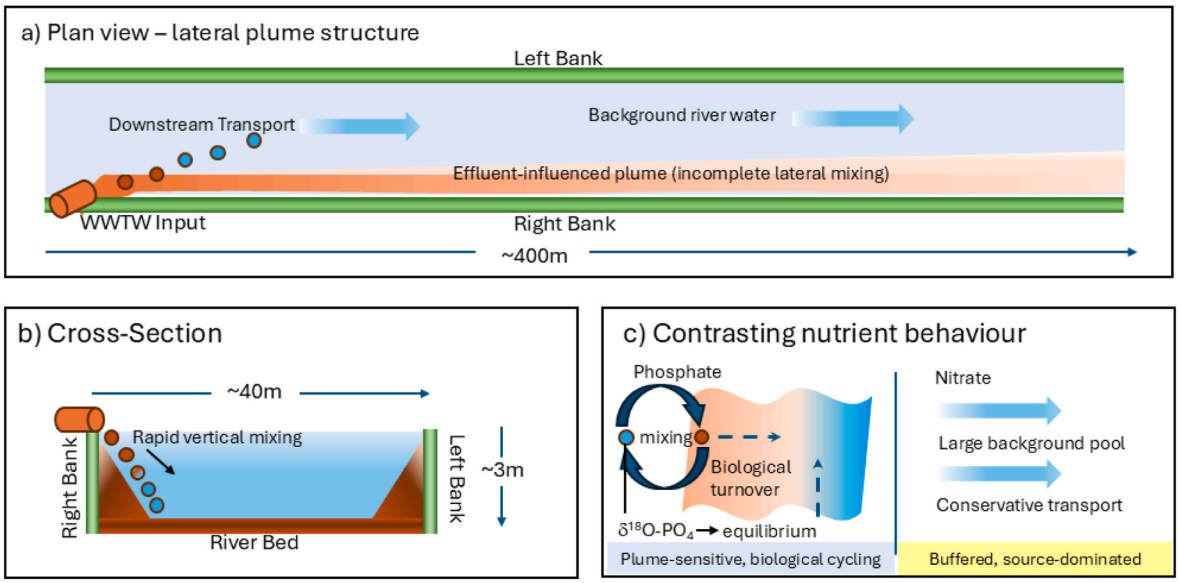

Fig. 7. Conceptual model of nutrient behaviour downstream of a wastewater discharge in a shallow, laterally heterogeneous river. Blue circles represent mixing and red circles biological cycling. (a) Plan-view schematic showing a bank-attached effluent plume transported downstream with incomplete lateral mixing. (b) Cross-section showing relatively rapid vertical mixing but slower lateral exchange, such that plume-influenced water occupies the near-bank part of the channel while remaining laterally structured. (c) Contrasting nutrient responses, with phosphate showing greater sensitivity to plume interception and biological isotope resetting, and nitrate behaving more conservatively because of buffering by the background nitrate pool. (For interpretation of the references to color in this figure legend, the reader is referred to the Web version of this article.)

contrast, displayed stronger spatial structure because the background phosphate pool was smaller and because $\delta^{18}O\text{-}PO_4$ is sensitive to both source mixing and subsequent biological isotope resetting. Plume interception therefore produced a more detectable and spatially variable phosphate signal than was observed for nitrate.

Recognition of this plume structure provides the physical framework for interpreting both the end-member mixing calculations and the isotope systematics. Mixing between effluent and river water occurs during downstream transport, but because lateral exchange remained incomplete over this reach, the resulting composition was not uniform across the channel. Each sample therefore represents the local mixture at that sampling position rather than a laterally averaged river signal. Without explicit consideration of this heterogeneity, isotope patterns may be over-interpreted as biogeochemical transformation when they partly reflect hydrodynamic structure.

5.2. Phosphate isotope behaviour: mixing, end-member uncertainty and possible phosphate isotope resetting

The phosphate oxygen isotope data indicate that local plume mixing was an important control on the observed spatial pattern in $\delta^{18}O\text{-}PO_4$. In the near field of the WwTW input, several $\delta^{18}O\text{-}PO_4$ values fell between those of the upstream river and the measured effluent sample, indicating that conservative end-member mixing provides a first-order explanation for the initial isotopic shift (Gooddy et al., 2018; Gruau et al., 2005). The two-end-member model suggests that approximately 20–55% of the local dissolved inorganic phosphate pool may have been derived from the effluent at plume-influenced sampling points, depending on lateral position. These values should be interpreted as apparent local effluent fractions for the sampled water masses, rather than as reach-averaged contributions to river phosphate.

The interpretation of $\delta^{18}O\text{-}PO_4$ is complicated by the fact that the upstream river phosphate was already close to the calculated temperature-dependent equilibrium composition of approximately 17.2‰. Conservative mixing between this near-equilibrium river phosphate and isotopically lighter effluent phosphate can therefore generate intermediate values that move towards the upstream river composition as the effluent contribution decreases. For this reason, proximity to the calculated equilibrium value cannot by itself be taken as proof of post-discharge biological isotope exchange. Instead, the equilibrium comparison is used here as an interpretive reference alongside the mixing model, lateral sampling position and phosphorus concentration data.

Several downstream samples were close to the calculated equilibrium composition, while some plume-influenced samples were displaced from it. This pattern is consistent with a combination of conservative mixing and biological isotope resetting, but it does not define a simple monotonic downstream trend or allow a turnover rate to be calculated. The data show a spatial pattern in $\delta^{18}O\text{-}PO_4$ relative to measured end members and calculated equilibrium, but travel times and biological exchange rates were not directly measured. The approach towards equilibrium is therefore interpreted cautiously as evidence consistent with short-reach phosphate isotope resetting, rather than as a quantified rate of biological turnover.

The low $\delta^{18}O\text{-}PO_4$ value of 12.5‰ observed at approximately 220 m downstream requires separate consideration. This value falls below the measured effluent end member and therefore cannot be produced by conservative two-end-member mixing using the upstream and effluent samples collected during the survey. Several explanations are possible, including analytical uncertainty, an additional phosphorus source, local biogeochemical effects, interaction with particulate or colloidal phosphorus, short-term temporal variability in the effluent, or lateral heterogeneity within the plume. Analytical uncertainty alone is unlikely to explain the magnitude of the offset, given the duplicate precision of the $\delta^{18}O\text{-}PO_4$ measurements. A separate unrecognised phosphorus source cannot be excluded entirely, but the coincidence of the low isotope value with elevated TDP and TP supports interpretation as a plume-influenced water mass. The most likely explanation is therefore that the single effluent grab sample did not fully constrain the isotopic variability of wastewater-derived phosphate entering or moving through the reach. The 220 m sample is therefore treated primarily as evidence of end-member and plume heterogeneity, rather than as part of a general downstream equilibration trend.

The contrasting behaviour of SRP, TDP and TP also indicates that phosphorus transport cannot be treated as a single homogeneous dissolved pool. The $\delta^{18}O\text{-}PO_4$ measurements represent phosphate isolated from filtered samples and are most directly related to the dissolved inorganic phosphate fraction. However, the greater spatial variability in TP and TDP suggests that particulate or colloidal phosphorus also contributed to the plume signal. This may help explain why phosphorus showed stronger spatial structure than nitrate, which was present almost entirely as dissolved nitrate and was strongly buffered by the large background nitrate pool. The isotope interpretation therefore applies specifically to the dissolved phosphate fraction, while the wider phosphorus concentration patterns also reflect particulate and colloidal transport.

Abiotic processes are unlikely to provide a better explanation for samples approaching the calculated equilibrium composition. Fractionation of phosphate oxygen isotopes during interaction with mineral surfaces, particularly iron oxides, has been demonstrated experimentally (Jaisi et al., 2010). However, such processes do not generally drive dissolved phosphate towards a temperature-dependent equilibrium with ambient water. In natural aquatic systems, oxygen isotope exchange between phosphate and water is primarily associated with enzymatically mediated biological reactions (Blake et al., 2005; McLaughlin et al., 2013). The phosphate isotope data are therefore consistent with some biological isotope resetting within the reach, but the strength of this inference is limited by the single-survey design, the lack of direct travel-time measurements and the incomplete characterisation of effluent end-member variability.

Overall, the phosphate isotope data show that $\delta^{18}O\text{-}PO_4$ integrates information on local plume mixing, end-member variability and possible biological isotope resetting. The key implication is that $\delta^{18}O\text{-}PO_4$ values downstream of wastewater inputs cannot be interpreted using either conservative mixing or biological equilibration alone. Both need to be considered within the lateral plume structure of the receiving river, and with explicit recognition of uncertainty in the measured end-member compositions.

5.3. Background nitrate buffering and unresolved nitrogen transformations

The limited nitrate isotope response downstream of the WwTW reflects the strong buffering effect of the background nitrate pool. Nitrate nitrogen and oxygen isotope compositions are largely inherited during nitrate formation and tend to remain stable during transport unless nitrate is actively transformed or removed, for example by assimilation or denitrification. In this reach, the river contained a large background nitrate pool of approximately 40 mg NO_3^- L^{-1}. Although the WwTW effluent nitrate was chemically and isotopically distinct, its contribution was insufficient to produce a clear downstream shift in bulk river nitrate concentration or isotope composition under the sampled hydrological conditions.

This interpretation does not require the absence of nitrogen transformation within the reach. Rather, it indicates that any such processes were not expressed as a measurable reach-scale change in the bulk nitrate isotope signal. The large background nitrate pool would strongly dampen any isotopic effect associated with local nitrification, assimilation or denitrification. This is particularly important because ammonium showed greater spatial variability than nitrate, although at much lower absolute concentrations. Local NH_4^+ variability may indicate plume influence or short-reach nitrogen cycling, but without $\delta^{15}N\text{–}NH_4$ measurements, dissolved oxygen or redox data, and direct nitrification-

rate measurements, the role of effluent-derived NH_4^+ transformation cannot be resolved. DOC was not measured during this survey, so the potential role of wastewater-derived organic carbon in supporting local microbial nitrogen or phosphorus transformations could not be assessed directly.

The absence of coupled downstream enrichment in $\delta^{15}N–NO_3$ and $\delta^{18}O–NO_3$ indicates no detectable isotopic evidence for substantial denitrification over the sampled reach and hydrological conditions. Denitrification typically produces coupled increases in both isotope ratios as nitrate is progressively consumed (Böttcher et al., 1990; Sebilo et al., 2003, 2006; Seitzinger, 1988), but such a trend was not observed here. However, this does not rule out denitrification occurring at other times, in localised sediments, within slower-flowing marginal zones, or under different hydraulic or redox conditions. It also does not exclude nitrification or assimilation occurring at rates too small to be detected against the large background nitrate pool.

The laterally structured plume also means that nitrogen processing may not have been spatially uniform across the channel. Samples collected nearer the bank may have experienced different velocities, residence times, sediment contact or organic matter availability than mid-channel samples. Such spatial differences could influence local nitrogen transformations, but the sampling design was not intended to quantify hydraulic residence times or bank-specific processing rates. The nitrate isotope data should therefore be interpreted as showing no detectable reach-scale nitrate transformation signal, rather than demonstrating that nitrogen cycling was absent.

Overall, nitrate behaved much more conservatively than phosphate at the scale resolved by this survey. This difference reflects not only the dissolved nature of nitrate, but also the large background nitrate pool, which buffered any effluent-related or process-related isotope signal. In contrast, phosphate showed stronger spatial structure because the background phosphate pool was smaller, $\delta^{18}O\text{-}PO_4$ is more sensitive to biological isotope exchange, and wider phosphorus patterns may also include particulate or colloidal transport. The contrast between nitrate and phosphate therefore highlights that nutrient isotope responses downstream of wastewater inputs depend on both biogeochemical reactivity and the size and form of the background nutrient pool.

5.4. *Implications for monitoring and interpretation of wastewater-affected rivers*

The results of this study show that robust interpretation of nutrient behaviour downstream of wastewater discharges requires explicit consideration of both lateral mixing structure and nutrient-specific reactivity. Where effluent forms a laterally confined plume, the assumption of complete cross-sectional mixing may not be valid over short spatial scales, and different water masses can be transported downstream in parallel. Under these conditions, the chemical and isotopic composition of any individual sample reflects both longitudinal distance from the discharge and lateral position relative to the plume (Volkmar et al., 2011; Bowes et al., 2014). Measurements collected at a single downstream location may therefore not capture the full cross-channel variability in effluent influence.

This has direct implications for sampling design. Downstream monitoring of point-source inputs should not assume complete lateral mixing unless this has been demonstrated for the reach and flow conditions being sampled. Where the outfall is bank-side, or where plume persistence is likely, sampling at multiple lateral positions is preferable to reliance on a single mid-channel or bank-side sample. At a minimum, the lateral position of each sample should be recorded and interpreted as part of the chemical and isotope dataset. Where regulatory or investigative monitoring depends on representative downstream concentrations, additional hydraulic information, such as flow gauging, dye tracing, ADCP measurements or high-frequency sensor deployment, would help determine whether a sample represents local plume water or a more mixed river signal.

For phosphate, incomplete lateral mixing is particularly important because both concentration and $\delta^{18}O\text{-}PO_4$ can respond strongly to local plume interception. Samples collected within plume-influenced water may capture phosphate that is chemically enriched and isotopically distinct from the background river pool, whereas samples collected outside the plume may better represent upstream or more fully mixed river conditions. Phosphate oxygen isotopes are therefore most useful where the aim is to evaluate the interaction between source mixing and biological cycling, but they should be interpreted alongside phosphorus fractions, end-member composition and hydrodynamic context. In particular, single effluent grab samples may not fully characterise end-member variability, so repeated effluent sampling or sensitivity analysis should be considered where quantitative source fractions are required.

In contrast, nitrate showed little measurable response over the same reach. Its concentration was dominated by a large background nitrate pool, and its isotope composition was not strongly perturbed by the effluent input under the sampled hydrological conditions. This does not exclude local nitrogen transformations, but it means that nitrate isotope signals may be difficult to interpret below wastewater inputs where the background nitrate pool is large relative to the effluent contribution. Under such conditions, ammonium, dissolved oxygen, DOC, redox conditions, $\delta^{15}N–NH_4$ or high-frequency concentration measurements may provide useful complementary information.

More generally, the study highlights that the downstream distance required for complete mixing should not be assumed to be fixed. It will vary with river flow, discharge rate, channel width, depth, turbulence, outfall position and bank geometry. The plume in this study remained laterally structured over the sampled 400 m reach, but the full downstream mixing length was not determined. Future studies and monitoring programmes would benefit from extending lateral sampling further downstream and linking isotope data with direct hydraulic measurements to determine when a point-source signal becomes cross-sectionally mixed.

From a management perspective, these results indicate that mitigation priorities downstream of WwTW discharges are likely to differ between nutrients. For phosphorus, the strong near-field response suggests that point-source controls at the discharge, together with an understanding of plume structure, are likely to be central to managing downstream impacts. For nitrate, the large background pool implies that catchment-scale loading may dominate over short-reach in-stream removal or localised outfall effects under similar conditions. In this WwTW context, nutrient behaviour therefore points to a practical distinction between near-field point-source management for phosphorus and broader catchment-scale management for nitrate.

6. Conclusions

This study shows that nutrient isotope behaviour downstream of a wastewater discharge can be strongly shaped by the interaction between lateral plume structure and nutrient-specific reactivity. Over the 400 m reach sampled here, the effluent did not behave as a fully cross-sectionally mixed input, but instead remained laterally structured within the channel. As a result, downstream nutrient concentrations and isotope compositions reflected both distance from the outfall and sampling position relative to the plume.

Within this hydrodynamic framework, phosphate and nitrate showed contrasting behaviour. Phosphate oxygen isotopes were sensitive to local plume interception, with near-field isotope compositions broadly consistent with first-order mixing between effluent and river phosphate. Further downstream, several $\delta^{18}O\text{-}PO_4$ values were close to the calculated temperature-dependent equilibrium composition, consistent with some possible biological isotope resetting of phosphate within the reach. However, because the upstream river phosphate was already close to equilibrium, and because travel times and isotope exchange rates were not directly measured, these patterns should be

interpreted as spatial evidence for mixing and isotope resetting rather than as quantified rates of phosphate turnover.

The low δ^{18}O-PO_4 value observed at approximately 220 m downstream fell outside the conservative mixing envelope defined by the measured upstream and effluent end members. This highlights the sensitivity of two-end-member calculations to end-member selection and supports the need to consider effluent variability and plume heterogeneity when interpreting phosphate isotope data downstream of point-source inputs.

In contrast, nitrate concentrations and isotope compositions (δ^{15}N–NO_3 and δ^{18}O–NO_3) showed little measurable response to the discharge over the same reach. The effluent nitrate signal was strongly buffered by the large background nitrate pool, and there was no detectable coupled isotopic enrichment indicative of substantial denitrification under the sampled hydrological conditions. This does not exclude local nitrogen transformations, but indicates that any such processes were not resolved in the bulk nitrate isotope signal during this survey.

More broadly, the results demonstrate that rivers receiving point-source inputs cannot always be interpreted as laterally well-mixed one-dimensional systems over short spatial scales. Integrating hydrodynamic context with multi-nutrient isotope measurements provides a stronger basis for interpreting nutrient behaviour in plume-affected river systems, particularly where source mixing, end-member uncertainty, background nutrient buffering and biological reactivity operate together.

Declaration of generative AI and AI-assisted technologies in the manuscript preparation process

During the preparation of this work, the author(s) used ChatGPT for language editing and improving clarity. The author(s) reviewed and edited the output as needed and take full responsibility for the content of the published article.

CRediT authorship contribution statement

Daren C. Gooddy: Conceptualization, Formal analysis, Funding acquisition, Investigation, Methodology, Project administration, Supervision, Writing – original draft, Writing – review & editing. **Michael J. Bowes:** Conceptualization, Funding acquisition, Investigation, Methodology, Writing – review & editing. **Alexandra V.E. O'Brien:** Data curation, Formal analysis, Investigation, Writing – review & editing. **David J.E. Nicholls:** Data curation, Formal analysis, Investigation, Writing – review & editing. **Andi C. Smith:** Formal analysis, Investigation, Methodology, Validation, Writing – review & editing. **James P. R. Sorensen:** Conceptualization, Funding acquisition, Investigation, Writing – review & editing. **Patrick Harrison:** Data curation, Investigation, Writing – review & editing. **Stefan Krause:** Conceptualization, Funding acquisition, Methodology, Writing – review & editing.

Declaration of competing interest

The authors declare that they have no known competing financial interests or personal relationships that could have appeared to influence the work reported in this paper.

Acknowledgements

The authors would like to thank Nick Everard, Cedric Laize and Ponnambalam Rameshwaran for assisting with sampling and characterising the river flow regime. This work was funded by The National Environment Isotope Facility (NEIF) under grant 2872.1024, and by NERC Large grant NE/X018830/1 SMARTWATER 'Diagnosing controls of pollution hot spots and hot moments and their impact on catchment water quality'. JPRS and PH publish with the permission of the Director BGS (NERC).

Data availability

Data will be made available on request.

References

Altabet, M.A., Wassenaar, L.I., Douence, C., Roy, R., 2019. A Ti(III) reduction method for one-step conversion of seawater and freshwater nitrate into N_2O for stable isotopic analysis of $^{15}N/^{14}N$, $^{18}O/^{16}O$ and $^{17}O/^{16}O$. Rapid Commun. Mass Spectrom. 33 (15), 1227–1239.

Böhlke, J.K., Denver, J.M., 1995. Combined use of groundwater dating, chemical, and isotopic analyses to resolve the history and fate of nitrate contamination in two agricultural watersheds, Atlantic coastal plain, Maryland. Water Resour. Res. 31, 2319–2339.

Blake, R.E., O'Neil, J.R., Garcia, G.A., 1997. Oxygen isotope systematics of biologically mediated reactions of phosphate: 1. Microbial degradation of organophosphorus compounds. Geochem. Cosmochim. Acta 61, 4411–4422.

Blake, R.E., O'Neil, J.R., Surkov, A.V., 2005. Biogeochemical cycling of phosphorus: insights from oxygen isotope effects of phosphoenzymes. Am. J. Sci. 305, 596–620.

Bowes, M.J., Armstrong, L.K., Harman, S.A., Wickham, H.D., Nicholls, D.J.E., Scarlett, P. M., Roberts, C., Jarvie, H.P., Old, G.H., Gozzard, E., Bachiller-Jareno, N., Read, D.S., 2018. Weekly water quality monitoring data for the river thames (UK) and its major tributaries (2009-2013): the thames initiative platform. Earth Syst. Sci. Data 10, 1637–1653.

Bowes, M.J., Jarvie, H.P., Naden, P.S., Old, G.H., Scarlett, P.M., Roberts, C., Armstrong, L.K., Harman, S.A., Wickham, H.D., Collins, A.L., 2014. Identifying priorities for nutrient mitigation using river concentration-flow relationships: the thames basin, UK. J. Hydrol. 517, 1–12.

Böttcher, J., Strebel, O., Voerkelius, S., Schmidt, H.L., 1990. Using isotope fractionation of nitrate-nitrogen and nitrate-oxygen for evaluation of microbial denitrification in a sandy aquifer. J. Hydrol. 114, 413–424.

Carpenter, S.R., Caraco, N.F., Correll, D.L., Howarth, R.W., Sharpley, A.N., Smith, V.H., 1998. Nonpoint pollution of surface waters with phosphorus and nitrogen. Ecol. Appl. 8, 559–568.

Chang, S.J., Blake, R.E., 2015. Precise calibration of equilibrium oxygen isotope fractionations between dissolved phosphate and water from 3 to 37 °C. Geochem. Cosmochim. Acta 150, 314–329.

Davies, C.L., Surridge, B.W.J., Gooddy, D.C., 2014. Phosphate oxygen isotopes within aquatic ecosystems: global data synthesis and future research priorities. Sci. Total Environ. 496, 563–575.

Eisenreich, S.J., Bannerman, R.T., Armstrong, D.E., 1975. A simplified phosphorus analytical technique. Environ. Lett. 9, 45–53.

Gooddy, D.C., Bowes, M.J., Lapworth, D.J., Lamb, A.L., Williams, P.J., Newton, R.J., Davies, C.L., Surridge, B.W.J., 2018. Evaluating the stable isotope composition of phosphate oxygen as a tracer of phosphorus from waste water treatment works. Appl. Geochem. 95, 139–146.

Gooddy, D.C., Lapworth, D.J., Bennett, S.A., Heaton, T.H.E., Williams, P.J., Surridge, B. W.J., 2016. A multi-stable isotope framework to understand eutrophication in aquatic ecosystems. Water Res. 88, 623–633.

Gruau, G., Legeas, M., Riou, C., Gallacier, E., Martineau, F., Henin, O., 2005. The oxygen isotope composition of dissolved anthropogenic phosphates: a new tool for eutrophication research? Water Res. 39, 232–238.

Hilton, J., O'Hare, M., Bowes, M.J., Iwan Jones, J., 2006. How green is my river? A new paradigm of eutrophication in rivers. Sci. Total Environ. 365, 66–83.

Jaisi, D.P., Blake, R.E., Kukkadapu, R.K., 2010. Fractionation of oxygen isotopes in phosphate during its interaction with iron oxides. Geochem. Cosmochim. Acta 74, 1309–1319.

Jarvie, H.P., Neal, C., Withers, P.J.A., 2006. Sewage-effluent phosphorus: a greater risk to river eutrophication than agricultural phosphorus. Sci. Total Environ. 360, 246–253.

Kendall, C., 1998. Tracing nitrogen sources and cycling in catchments. In: Kendall, C., McDonnell, J.J. (Eds.), Isotope Tracers in Catchment Hydrology. Elsevier, Amsterdam, pp. 519–576.

Kendall, C., Elliott, E.M., Wankel, S.D., 2007. Tracing anthropogenic inputs of nitrogen to ecosystems. In: Michener, R., Lajtha, K. (Eds.), Stable Isotopes in Ecology and Environmental Science, second ed. Blackwell, pp. 375–449.

Matiatos, I., Wassenaar, L.I., Monteiro, L.R., Venkiteswaran, J.J., Gooddy, D.C., Boeckx, P., Sacchi, E., Yue, F.-J., Michalski, G., Alonso-Hernandez, C., Biasi, C., Bouchaou, L., Edirisinghe, N.V., Fadhullah, W., Fianko, J.R., Garcia-Moya, A., Kazakis, N., Li, S.-L., Luu, M.T.N., Priyadarshanee, S., Re, V., Rivera, D.S., Romanelli, A., Sanyal, P., Tamooh, F., Trinh, D.A., Walters, W., Welti, N., 2021. Global patterns of nitrate isotope composition in rivers and adjacent aquifers reveal reactive nitrogen cascading. Commun. Earth Environ. 2, 52.

McLaughlin, K., Kendall, C., Silva, S., Young, M., Paytan, A., 2006. Phosphate oxygen isotope ratios as a tracer for sources and cycling of phosphate in North San Francisco Bay, California. J. Geophys. Res. Biogeosci. 111, G03003.

McLaughlin, K., Young, M.B., Paytan, A., Kendall, C., 2013. The oxygen isotopic composition of phosphate: a tracer for phosphate sources and cycling. In: Application of Isotope Techniques for Assessing Nutrient Dynamics in River Basins. IAEA-TECDOC-1695, Vienna, pp. 93–111.

Murphy, J., Riley, J.P., 1962. A modified single solution method for the determination of phosphate in natural waters. Anal. Chim. Acta 27, 31–36.

Neal, C., Neal, M., Wickham, H., 2000. Phosphate measurement in natural waters: two examples of analytical problems associated with silica interference using phosphomolybdic acid methodologies. Sci. Total Environ. 251 (252), 511–522.
Nisbeth, C.S., Tamburini, F., Kidmose, J., Jessen, S., O'Connell, D.W., 2022. Analysis of oxygen isotopes of inorganic phosphate ($\delta^{18}O_p$) in freshwater: A detailedamethod description for obtaining oxygen isotopes of inorganic phosphate in environmental water samples. MethodsX 9, 101706.
Palmer-Felgate, E.J., Mortimer, R.J.G., Krom, M.D., Jarvie, H.P., 2010. Impact of point-source pollution on phosphorus and nitrogen cycling in stream-bed sediments. Environ. Sci. Technol. 44, 908–914.
Pfahler, V., Adu-Gyamfi, J., Pistocchi, C., Tamburini, F., Bauke, S., 2024. Stable oxygen isotope composition of phosphates to investigate phosphorus cycling in the soil-plant continuum. In: Adu-Gyamfi, J., et al. (Eds.), Tracing the Sources and Fate of Contaminants in Agroecosystems. Springer, Cham.
Sebilo, M., Billen, G., Grably, M., Mariotti, A., 2003. Isotopic composition of nitrate-nitrogen as a marker of riparian and benthic denitrification at the scale of the whole seine river system. Biogeochemistry 63, 35–51.
Sebilo, M., Billen, G., Mayer, B., Billiou, D., Grably, M., Garnier, J., Mariotti, A., 2006. Assessing nitrification and denitrification in the seine river and estuary using chemical and isotopic techniques. Ecosystems 9, 564–577.
Seitzinger, S.P., 1988. Denitrification in freshwater and coastal marine ecosystems: ecological and geochemical significance. Limnol. Oceanogr. 33, 702–724.
Tonderski, K., Andersson, L., Lindström, G., St Cyr, R., Schönberg, R., Taubald, H., 2017. Assessing the use of δ18O phosphate as a tracer for catchment phosphorus sources. Sci. Total Environ. 607–608, 1–10.
Venkiteswaran, J.J., Boeckx, P., Gooddy, D.C., 2019. Towards a global interpretation of dual nitrate isotopes in surface waters. J. Hydrol. X 4, 100037.
Volkmar, E.C., Dahlgren, R.A., Stringfellow, W.T., Henson, S.S., Borglin, S.E., Kendall, C., Van Nieuwenhuyse, E.E., 2011. Using Lagrangian sampling to study water quality during downstream transport in the San Luis drain, California, USA. Chem. Geol. 283, 68–77.
von Sperber, C., Pistocchi, C., Weiler, M., Tamburini, F., 2023. Oxygen isotope ratios of phosphates in the soil-plant system: limitations and future developments. Eur. J. Soil Sci. 74, e13434.
Wang, Z., Sun, F., Guo, Q., Gooddy, D.C., Wu, F., 2024. Global scale identification of catchment phosphorus source shifts with urbanization: a phosphate oxygen and Bayesian mixing model approach. Water Res. 250, 121026.
Wang, Z., Tian, L., Zhao, C., Du, C., Zhang, J., Sun, F., Tekleab, T.Z., Wei, R., Gooddy, D. C., Guo, Q., 2023. Source partitioning using phosphate oxygen isotopes and multiple models in a large catchment. Water Res. 244, 120382.
Wassenaar, L.I., 1995. Evaluation of the origin and fate of nitrate in the Abbotsford aquifer using the isotopes of ^{15}N and ^{18}O in NO_3^-. Appl. Geochem. 10, 391–405.
Water Framework Directive (WFD), Council of European Communities, 2000. Establishing a framework for community action in the field of water policy (2000/60/EC). Off. J. Europ. Comm. L327.
Young, M.B., McLaughlin, K., Kendall, C., Stringfellow, W., Rollog, M., Elsbury, K., Donald, E., Paytan, A., 2009. Characterizing the oxygen isotopic composition of phosphate sources to aquatic ecosystems. Environ. Sci. Technol. 43, 5190–5196.